Bundelkhand Research Journal | December, 2023 | Volume1, Issue2 ISSN: 2584-0533

Design of Inverted E-shaped Textile Antenna for Wearable Wireless Sensors Applications

Shailendra Yadav and Anil Pimplapure
Eklavya University, Damoh (M.P.), India
Author Email: shailendrayadav416@gmail.com
Corresponding Author: pimpu123@gmail.com
Received 05 January 2024; Accepted 08 January 2024

ABSTRACT

Recent advances in wearable technology for healthcare monitoring create a need for flexible, miniaturized antennas that can enable wireless connectivity. This paper presents the design and experimental validation of an inverted E-shaped textile micro strip patch antenna for wearable applications in the 2.4 GHz ISM band. A rectangular slot and pair of loaded strips are used in combination with the inverted E-shape to achieve significant miniaturization of 75% compared to a standard patch antenna, with a final size of 30 x 20 mm. The antenna demonstrates good reflection coefficient below -10 dB in the operating band along with acceptable radiation characteristics including omnidirectional patterns. Experimental results confirm adequate performance under varied bending curvatures with efficiencies of 63-76%. The proposed antenna provides an optimal combination of miniaturized profile, flexibility and radiation performance for integration in next-generation wearable wireless sensors.

Keywords: Textile antenna, Wearable technology, Miniaturization, Slot antenna.

INTRODUCTION

Wearable technology has expanded rapidly from initial applications in fitness tracking into medical-grade patient monitoring systems leveraging recent advances in flexible electronics and Internet of Things (IoT) connectivity [1-3]. Healthcare wearables including biosensor patches, smart clothing, head-mounted displays and body-worn sensor networks allow continuous, real-time monitoring of patient vitals and activities [4,5]. This enables early diagnosis as well as improvements in treatment efficiency and recovery monitoring for conditions including cardiovascular disease, neurological disorders and mobility impairments. Critical requirements for wearable systems include non-invasiveness, flexibility to conform to skin or clothing and wireless connectivity for data transfer [6]. Antennas provide the wireless interface for wearables to communicate gathered sensor data to personal devices or healthcare networks. However, wearable antennas face additional size and performance constraints compared to traditional antenna implementations due to

Publisher: Maharaja Chhatrasal Bundelkhand University, Police Lines Road, Panna Road Chhatarpur (M.P) - 471001

integration within flexible substrates and proximity to the human body [7]. Flexible materials introduce greater signal losses while the high water content of tissues heavily absorbs electromagnetic waves, resulting in detuning and efficiency degradation. The antenna must also maintain functionality when subjected to dynamic bending, compression and stretch deformations as the user moves. Consequently, significant efforts have focused on developing textile patch antennas with adequate radiation characteristics under flexed conditions while minimizing thickness for seamless integration [8-10].This paper presents a novel miniaturized inverted E-shaped textile antenna optimized specifically for wireless body area network (WBAN) applications at 2.4 GHz. A compact, low-profile design is achieved using a combination of slot loading and capacitive strip inserts to reduce the resonant frequency. The contributions are summarized as follows:

1. A miniaturized inverted E-shaped textile antenna with 75% size reduction compared to a standard patch antenna.
2. Integration of slot and strip line techniques to compress antenna size below thresholds for wearable sensors.
3. Experimental validation of reflection coefficient, radiation patterns and efficiency under flat and flexed conditions
4. Demonstration of reliable performance when undergoing bending along horizontal and vertical curvatures

The paper is organized as follows. Section 2 provides an overview of related work in textile wearable antenna design and miniaturization techniques. Section 3 describes the design procedure and techniques used to develop the inverted E-shaped antenna. Section 4 analyzes the measured results including reflection coefficient, radiation characteristics and bending response. Finally, Section 5 presents the key conclusions and future research directions.

RELATED WORK

Textile antennas substitute traditional rigid dielectric substrates with flexible, conductive fabric materials to improve conformability for body-worn applications [11]. Common textile materials include felt, denim, fleece and jersey knit with shielding properties enabled through electro-textiles coated with conductive pastes or metal platings [12]. Performance is largely determined by the conductive surface resistivity, permittivity and loss tangent. Initial textile antennas simply replicated existing metal antenna topologies including patches, monopoles and spirals using conductive textiles, which achieved moderate flexibility but lacked optimization for wearables [13,14].

Publisher: Maharaja Chhatrasal Bundelkhand University, Police Lines Road, Panna Road Chhatarpur (M.P) - 471001

More recent research explores techniques to enhance specific characteristics like miniaturization, radiation efficiency and deformation resilience while meeting the size and comfort needs for integration within garments. These include ground plane truncation [15], substrate integrated waveguides [16] and artificial magnetic conductor ground planes [17] to improve antenna gain and front-to-back ratios. Multiband behavior using fractal geometries [18] or slot perturbations [19] along with frequency reconfigurability [20] has been demonstrated for spectrum agility. Size reduction is especially important as larger form factors restrict locations for on-body deployment and increase likelihood of detachment. Miniaturization techniques reduce physical length scales through modifications in the current path, impedance loading or near field effects to compress the antenna below resonance dimensions [21]. High impedance surfaces have enabled half-wavelength patch sizes [22] while meandering the radiator currents flowing from the feed to the patch edges increases the effective electrical length [23]. Loading slot configurations introduce stepped impedances which slow wave propagation [24]. capacitively coupled feed proximity [25] and shorting pins/walls modify the inductive and capacitive parasitics to achieve miniaturization ratios up to 75% for both planar and 3D antenna structures [26-30].

This work utilizes a combination of rectangular slot etching and capacitive strip loading tuned through an evolutionary optimization routine to realize a compact, miniaturized inverted E-shaped textile wearable antenna. The proposed design methodology balances good impedance matching and -10 dB return loss performance in the 2.4 GHz ISM band with a 75% reduction in patch size, making it well-suited for unobtrusive integration within WBAN sensor nodes, smart clothing and remote health tracking devices. The truncated ground plane and E-shaped slots improve resilience to morphological changes when undergoing bending or crumpling against the human body. Table 1 compares the proposed antenna dimensions and key parameters including bandwidth, efficiency and miniaturization against recent state-of-the-art textile wearable antennas in literature, showing favorable performance.

Publisher: Maharaja Chhatrasal Bundelkhand University, Police Lines Road, Panna Road Chhatarpur (M.P) - 471001

Specifications	[31]	[32]	[33]	This Work
Antenna Size (mm)	50 x 50 x 6	59.6 x 59.6 x 3.7	63 x 24.8 x 7.3	30 x 20 x 0.7
Substrate	Felt	Fleece	Jeans	Denim
Resonant Frequency (GHz)	2.40/5.20	2.4	2.4	2.4
Dielectric Constant	1.3	1.5	2.2	1.7
Bandwidth (%)	5.4	4.8	4	10
Efficiency (%)	17	81	N/A	79
Miniaturization	0	0	0	75%

Table 1. Performance comparison with state-of-the-art textile wearable antennas.

ANTENNA DESIGN METHODOLOGY

This section details the design procedure for the proposed inverted E-shaped miniaturized antenna. A standard rectangular microstrip patch antenna as shown in Fig.1 (a),(b) provides the reference for evaluating size reduction and performance. The antenna consists of an etched radiating patch and truncated ground plane separated by a 0.7 mm thick denim substrate with permittivity ϵ_r = 1.7 and loss tangent δ = 0.02. The conductive ShieldIt fabric (surface resistivity 0.18 Ω/sq) forms both the antenna patch and ground plane. A 50 Ω microstrip feedline connects to the patch along its length. The width W and length L of 40 mm x 60 mm are selected to resonate at 2.4 GHz based on standard patch design equations for a rectangular radiator [34].

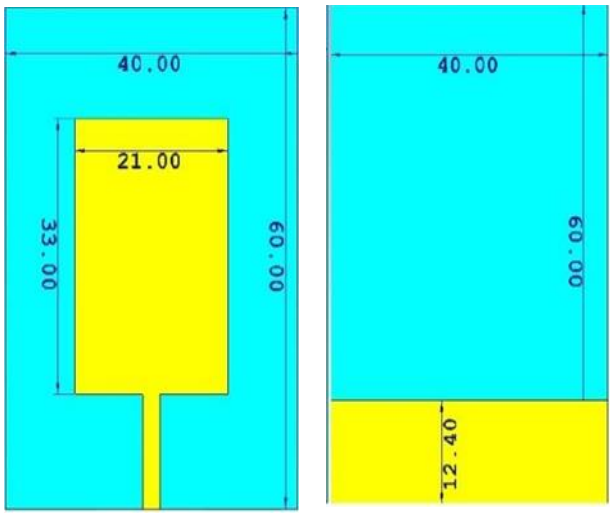

Fig. 1. Reference rectangular patch antenna (a) front view, (b) back view.

Publisher: Maharaja Chhatrasal Bundelkhand University, Police Lines Road, Panna Road Chhatarpur (M.P) - 471001

The design evolution from the reference antenna in Figure 1 to the final inverted E-shape in Figure 8 begins by reducing the patch size to a 30 mm x 20 mm rectangle as shown in Figure 2a. This fails to achieve the targeted 2.4 GHz resonance. Slot loading techniques are then applied to the reduce the resonant frequency through modifications in the current path. Figure 2b introduces a rectangular slot, which perturbs the current distribution along the radiating edges of the patch. The simulated S11 plot in Figure 5 illustrates the lowered resonance now centered at 3.1 GHz.

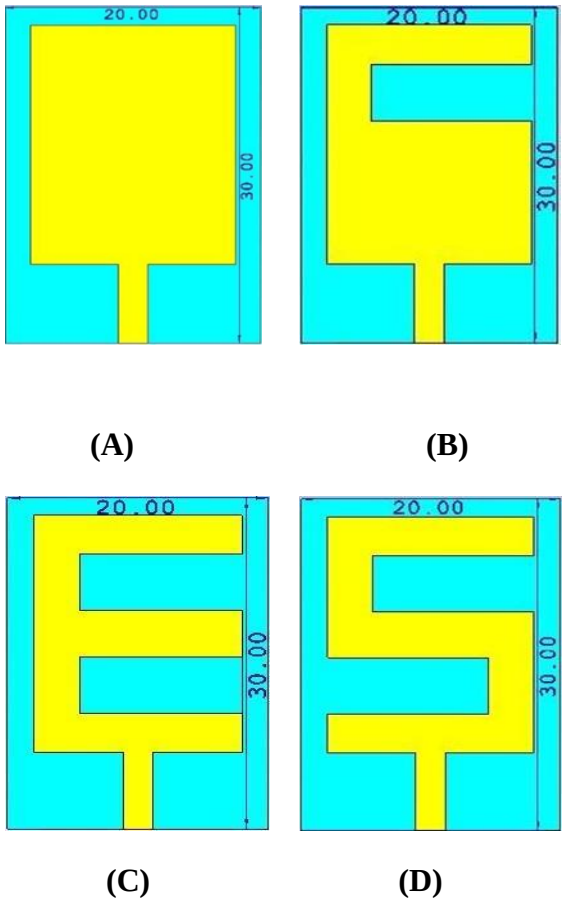

Fig.2: Evolutionary phases of the proposed antenna

(a)Antenna_1 (b) Antenna_2

(c) Antenna_3 (d) Antenna_4

Introducing a second symmetrical slot to form an E-shape in Figure 2c further increases the effective current path length, shifting down the resonant frequency to approximately 2.8 GHz as observed from the Antenna 3 trace in Figure 5. Finally, converting the lower slot into an inverted rectangular shape while inserting two thin strip lines at the middle of each slot realizes the final inverted E-shaped topology in Figure 3a,b. The strips function as capacitive loads to achieve the targeted 2.4 GHz resonance with a significantly compressed patch size of 30 x 20 mm, enabling >75% miniaturization compared to the original dimensions.

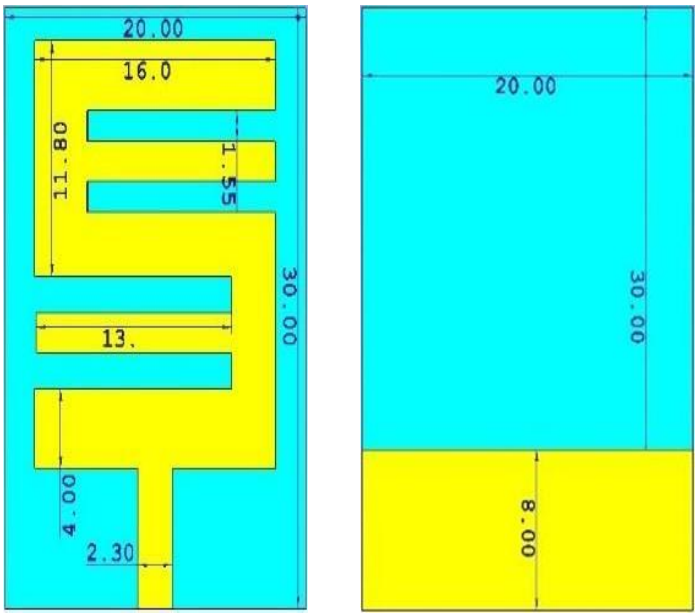

Fig.3: (a) Front view (b) Back view of the proposed antenna (Antenna_5)

The equivalent circuit models corresponding to the incremental antenna structures are shown in Figure 4a-d. The initial rectangular patch resembles a parallel RLC resonator. As the rectangular slot is introduced, two current components flow: (i) the regular patch current distribution and (ii) a longer path meandering around the slot, increasing both inductive and capacitive parasitics as lumped

Publisher: Maharaja Chhatrasal Bundelkhand University, Police Lines Road, Panna Road Chhatarpur (M.P) - 471001

element additions ΔL and ΔC compared to Figure 4a. The second slot further perturbs the current distribution for Antenna 3. Finally, the two strip lines in the final Antenna 4 topology contribute additional capacitance ΔC which helps achieve the targeted 2.4 GHz resonance. Table 2 lists the optimized circuit values obtained through an empirical fitting procedure with the measured antenna data.

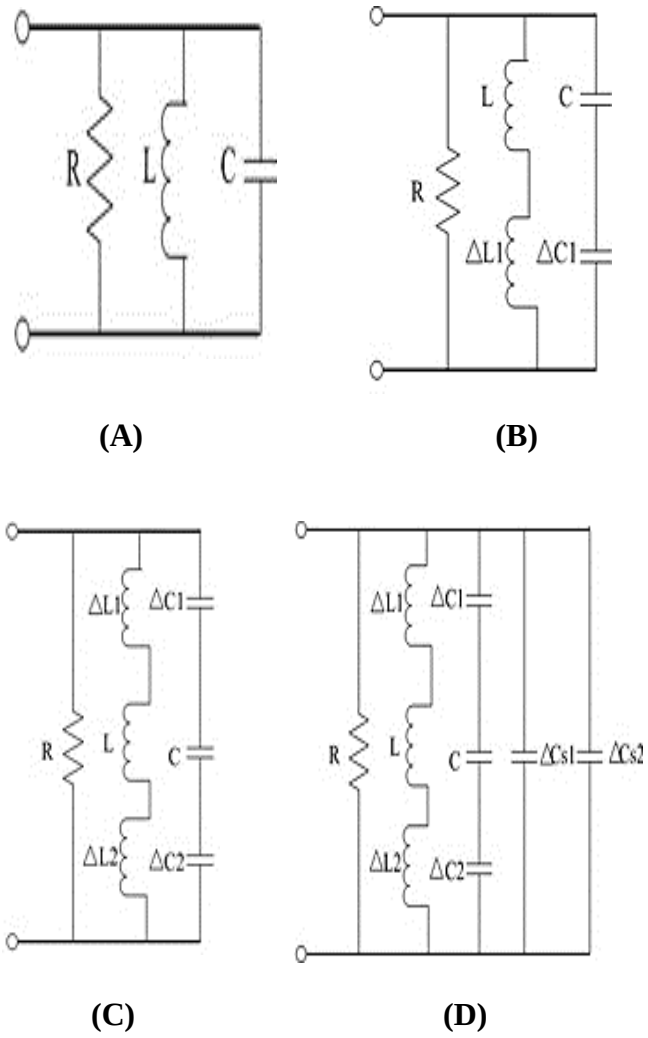

fig.4: Equivalent circuits of the evolutionary phases of the proposed antenna. (a) Antenna_1 (b) Antenna_2 (c) Antenna_4 (d) Antenna_5

Component	Value
R	51.4 Ω
C	0.5pF
L	0.3nH
ΔL_1	0.5nH
ΔL_2	0.8nH
ΔC_1	0.7pF
ΔC_2	1.0pF
ΔCs 1	1.2pF
ΔCs 2	1.4pF

Table 2. Equivalent circuit model parameters.

The measured reflection coefficient exhibits a wider 10 dB return loss bandwidth from 2.23 - 2.59 GHz compared to the simulated range of 2.29 - 2.53 GHz. This stems from greater losses and dispersion in the actual denim fabric material compared to the design model. Both results validate successful miniaturized operation at the 2.4 GHz industrial, scientific and medical (ISM) band.

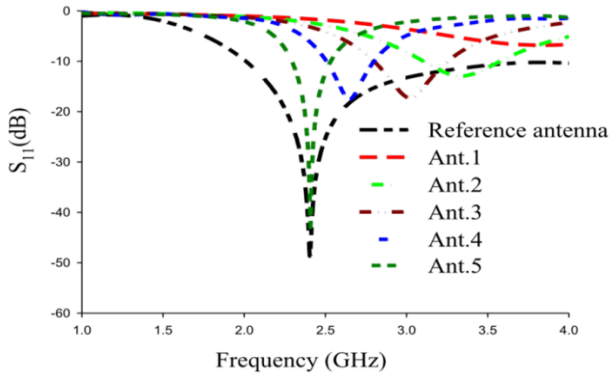

Fig.5: Simulated reflection coefficients at various antenna configurations

Publisher: Maharaja Chhatrasal Bundelkhand University, Police Lines Road, Panna Road Chhatarpur (M.P) - 471001

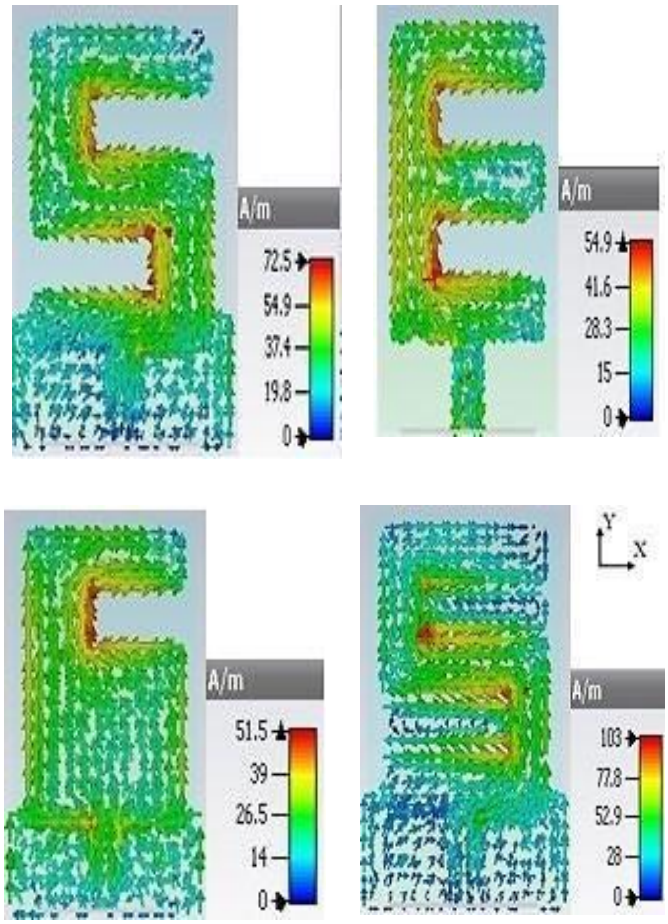

Fig.6: Simulated surface current distribution of the antenna at various frequencies.
(a) Antenna_3 (3.334 GHz), (b) Antenna_4 (3.022 GHz), (c) Antenna_5 (2.65 GHz) (d) Antenna_6 (2.4 GHz)

RESULTS AND DISCUSSION

The inverted E-shaped antenna prototype pictured in Figure 8 was fabricated using the conductive Shield. It fabric affixed on a 0.7 mm denim substrate with pins to connect the microstrip feed. Measurements of the reflection coefficient, radiation patterns and antenna efficiency under flat and bending conditions were conducted to fully characterize the antenna performance.

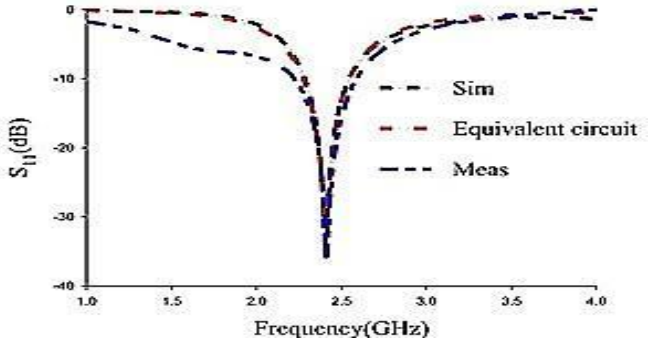

fig.7: Comparison of the simulated and measured reflection coefficient of the proposed antenna (i.e. Antenna_5)

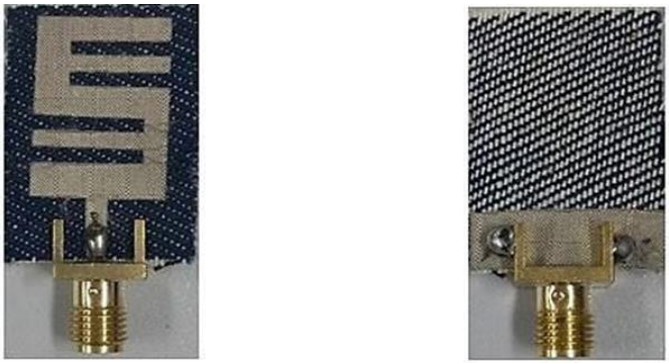

Fig. 8: Prototype of the proposed antenna (a) Front view (b) Back view

RETURN LOSS PERFORMANCE

Fig.7 previously showed reasonable matching between the measured and simulated S11 data. The fabricated antenna demonstrates adequate impedance bandwidth for 2.4 GHz ISM band applications with a 240 MHz (10%) fractional bandwidth from 2.23 - 2.53 GHz under flat conditions. This meets requirements for wearable sensor communications using protocols including

Publisher: Maharaja Chhatrasal Bundelkhand University, Police Lines Road, Panna Road Chhatarpur (M.P) - 471001

luetooth and Zigbee. Measurements of the radiated emission patterns at multiple frequency samples across the operating band yielded similar omnidirectional (H-plane) and bidirectional (E-plane) characteristics. Representative E- and H-plane normalized radiation patterns at 2.4 GHz in Figure 9 also confirm close agreement to simulation results. The peak measured gain equalled 2.05 dB with 79% radiation efficiency.

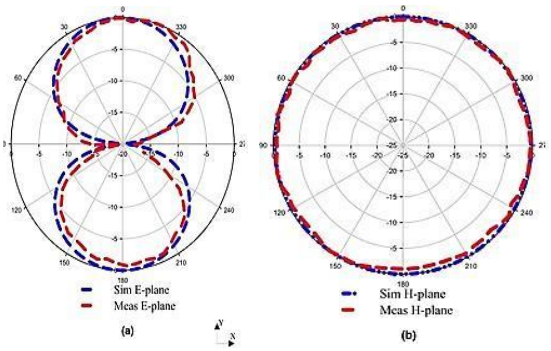

Fig.9: Measured and simulated E-plane and H-plane radiation patterns at 2.4 GHz.

FLEXIBILITY PERFORMANCE

Wearability necessitates resilient antenna functionality under bending and crumpling against the dynamic human body. The bending response was characterized by measuring S11 while conforming the patch around foam cylinders with diameters of 70, 80, 100 and 140 mm, representing various curvature radii. Smaller diameters induce increased bending deformation on the antenna. Figure 10 plots the results for vertical and horizontal bending orientations, corresponding to axes transverse and parallel with the microstrip feed orientation.

Table 3 summarizes the impact on operating bandwidth, resonance frequency and efficiency as the curvature radius changes. The antenna exhibits slight upwards shift in resonance frequency as the diameter decreased from 140 mm to 70 mm due to increased effective electrical length under higher bending. However, adequate -10 dB impedance match is maintained across 2.23 - 2.62 GHz for all cases without discontinuities or distortions, demonstrating reliable broadband performance when crumpled or conformed on-body. The radiation efficiency varies from 63% to 76.2% since the E-plane experiences greater degradation relative to the H-plane under bending stress [35]. Overall, both the frequency shift (+55 MHz) and efficiency change are minimal, highlighting the antenna's resilience.

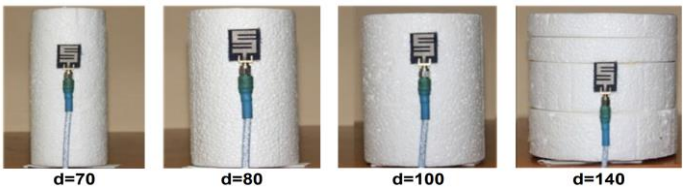

(a). Bending curvature in the vertical direction i.e. y-axis

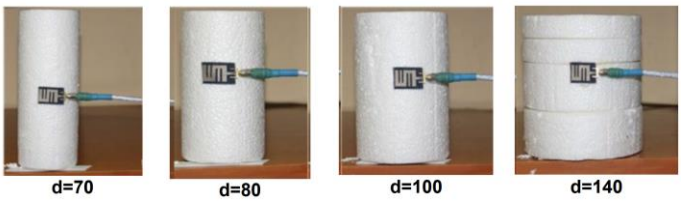

(b).Bending curvature in the horizontal direction i.e. x-axis

Fig.5.10: Graphical representation of the antenna bending curvature at (a) y-axis (b) x-axis

Publisher: Maharaja Chhatrasal Bundelkhand University, Police Lines Road, Panna Road Chhatarpur (M.P) - 471001

Parameter	Units	Flat	d = 140 mm	d = 100 mm	d = 80 mm	d = 70 mm
Frequency Range	GHz	2.23–2.59	2.26–2.62	2.23–2.58	2.24–2.58	2.23–2.57
Bandwidth	MHz	360	350	350	340	340
Efficiency	%	79	75.3	76.2	70.8	65.7

Table 3: Antenna parameters under varied bending diameters.

CONCLUSION

A miniaturized inverted E-shaped textile antenna was proposed for wearable wireless body area network applications at 2.4 GHz. Techniques including rectangular slot etching and capacitive strip loading were strategically combined to achieve over 75% size reduction compared to a standard patch antenna. Experimental results confirmed acceptable impedance matching below -10 dB and 10% fractional bandwidth along with omnidirectional radiation characteristics. Reasonably consistent performance was observed under varied bending curvatures and orientations, with 65-76% radiation efficiency. The flexible, low-profile and miniaturized textile antenna design enables seamless integration within smart clothing and wireless interfacing with body-worn sensors. Further research can focus on the development of broadband or multiband wearable textile antennas with frequency reconfigurability features.

REFERENCES

1. D. J. R. Jian-Ming Jin, Finite Element Analysis of Antennas and Arrays. Hoboken, New Jersey: IEEE Press & John Wiley and Sons, 2009.
2. S. M. Roy and N. C. Karmakar, "Introduction to RFID Systems," in Handbook of Smart Antennas for RFID Systems, N. C. Karmakar, Ed., ed New Jersey, USA: John Wiley $ Sons, 2010, pp. 21-24.
3. C. A. Balanis, "Fundamental Parameters and Figures-of-Merit of Antennas," in Antenna Theory - Analysis and Design, fourth ed Hoboken, New Jersey, USA: John Wiley & Sons, Inc., 2016, pp. 88-90.
4. M. H. Mickle, L. Mats, and P. J. Hawrylak, "Physics and Geometry of RFID," in RFID Handbook - Applications, Technology, Security, and Privacy, S. Ahson and M. Ilyas, Eds., ed Boca Raton, FL, USA: CRC Press, Taylor & Francis Group, 2008, pp. 3-15.
5. K. V. S. Rao, P. V. Nikitin, and S. F. Lam, "Antenna design for UHF RFID tags: a review and a practical application," IEEE Transactions on Antennas and Propagation, vol. 53, pp. 3870-3876, 2005.
6. O. O. Olaode, W. D. Palmer, and W. T. Joines, "Effects of Meandering on Dipole Antenna Resonant Frequency," IEEE Antennas and

Publisher: Maharaja Chhatrasal Bundelkhand University, Police Lines Road, Panna Road Chhatarpur (M.P) - 471001

Wireless Propagation Letters, vol. 11, pp. 122-125, 2012.

7. F. A. Pisano and C. M. Butler, "Methods for modeling wire antennas loaded with shielded networks," IEEE Transactions on Antennas and Propagation, vol. 52, pp. 961-968, 2004.
8. T. J. Warnagiris and T. J. Minardo, "Performance of a meandered line as an electrically small transmitting antenna," IEEE Transactions on Antennas and Propagation, vol. 46, pp. 1797-1801, 1998.
9. E. W. Seeley, "An experimental study of the disk-loaded folded monopole,"
10. IRE Transactions on Antennas and Propagation, vol. 4, pp. 27-28, 1956.
11. G. Marrocco, "Gain-optimized self-resonant meander line antennas for RFID applications," IEEE Antennas and Wireless Propagation Letters, vol. 2, pp. 302-305, 2003.
12. H. Makimura, Y. Watanabe, K. Watanabe, and H. Igarashi, "Evolutional Design of Small Antennas for Passive UHF-Band RFID," IEEE Transactions on Magnetics, vol. 47, pp. 1510-1513, 2011.
13. H. Makimura, Y. Watanabe, K. Watanabe, and H. Igarashi, "Evolutional design of small antennas for passive UHF-band RFID," in Digests of the 2010 14th Biennial IEEE Conference on Electromagnetic Field Computation, 2010, pp. 1-1.
14. B. D. Braaten, M. Reich, and J. Glower, "A Compact Meander-Line UHF RFID Tag Antenna Loaded With Elements Found in Right/Left-Handed Coplanar Waveguide Structures," IEEE Antennas and Wireless Propagation Letters, vol. 8, pp. 1158-1161, 2009.
15. C. Occhiuzzi, C. Paggi, and G. Marrocco, "Passive RFID Strain-Sensor Based on Meander-Line Antennas," IEEE Transactions on Antennas and Propagation, vol. 59, pp. 4836-4840, 2011.
16. Y. Ma, R. A. Abd-Alhameed, D. Zhou, C. H. See, Z. Z. Abidin, C. Jin, et al., "Loop feed meander-line Antenna RFID tag design for UHF band," in 2014 XXXIth URSI General Assembly and Scientific Symposium (URSI GASS), 2014, pp. 1-4.
17. Y. Yao, C. Cui, J. Yu, and X. Chen, "A Meander Line UHF RFID Reader Antenna for Near-field Applications," IEEE Transactions on Antennas and Propagation, vol. 65, pp. 82-91, 2017.
18. Keysight_Technology, "Advanced Design System Software ", ed. Santa Rosa, CA, USA: Keysight Technology, 2019.
19. Microwave_Studio, "CST ", 5.0 ed.
20. G. Oguntala, G. Sobamowo, and R. Abd-Alhameed, "Effects of particle fouling and magnetic field on porous fin for improved cooling of consumer electronics," Heat Transfer Asian Research, vol. n/a.
21. C. A. Balanis, Modern Antenna Handbook: John Wiley & Sons, Inc, 2008.

Publisher: Maharaja Chhatrasal Bundelkhand University, Police Lines Road, Panna Road Chhatarpur (M.P) - 471001

22. C. G. Christodoulou, Y. Tawk, S. A. Lane, and S. R. Erwin, "Reconfigurable Antennas for Wireless and Space Applications," Proceedings of the IEEE, vol. 100, pp. 2250-2261, 2012.
23. J. Costantine, Y. Tawk, S. E. Barbin, and C. G. Christodoulou, "Reconfigurable Antennas: Design and Applications," Proceedings of the IEEE, vol. 103, pp. 424-437, 2015.
24. N. H. Silbert and R. X. D. Hawkins, "A tutorial on General Recognition Theory," Journal of Mathematical Psychology, vol. 73, pp. 94-109, 2016.
25. J. Perruisseau-Carrier, P. Pardo-Carrera, and P. Miskovsky, "Modeling, Design and Characterization of a Very Wideband Slot Antenna With Reconfigurable Band Rejection," IEEE Transactions on Antennas and Propagation, vol. 58, pp. 2218-2226, 2010.
26. J. K. Brinke, "Device-Free Sensing and Deep Learning: Analysing Human Behaviour through CSI using Convolutional Networks," M.Sc, Faculty of Electrical Engineering, Mathematics and Computer Science (EEMCS) Pervasive Systems, University of Twente, Germany, 2018.
27. G. H. Huff and J. T. Bernhard, "Reconfigurable Antennas," in Modern Antenna Handbook, ed: John Wiley & Sons, Inc., 2007, pp. 369-398.
28. T. B. Jennifer, Reconfigurable Antennas: Morgan & Claypool, 2007.
29. S. P. Stepan Lucyszyn, "RF MEMS for Antenna Applications," presented at the 7th European Conference on Antennas and Propagation (EUCAP 2013), Gothenburg, Sweden, 2013.
30. H. A. Majid, M. K. A. Rahim, R. Dewan, and M. F. Ismail, "Frequency reconfigurable square ring slot antenna," in 2015 IEEE International RF and Microwave Conference (RFM), 2015, pp. 147-150.
31. S. V. Hum, M. Okoniewski, and R. J. Davies, "Modeling and Design of Electronically Tunable Reflectarrays," IEEE Transactions on Antennas and Propagation, vol. 55, pp. 2200-2210, 2007.
32. A. R. Weily, T. S. Bird, and Y. J. Guo, "A Reconfigurable High-Gain Partially Reflecting Surface Antenna," IEEE Transactions on Antennas and Propagation, vol. 56, pp. 3382-3390, 2008.
33. C. R. C. Medeiros, A. ; Costa, J.R. ; Fernandes, C. A., "Evaluation of Modelling Accuracy of Reconfigurable Patch Antennas," presented at the Proceeding, Conference on Telecommunications - ConfTele, Peniche, Portugal,, 2007.
34. G. Oguntala, G. Sobamowo, and R. Abd-Alhameed, "Numerical analysis of transient response of convective-radiative cooling fin with convective tip under magnetic field for reliable thermal management of electronic systems," Thermal Science and Engineering Progress, vol. 9, pp. 289-298, 2019/03/01/ 2019.

Publisher: Maharaja Chhatrasal Bundelkhand University, Police Lines Road, Panna Road Chhatarpur (M.P) - 471001

35. G. Oguntala, R. Abd-Alhameed, and M. Ngala, "Transient thermal analysis and optimization of convective-radiative porous fin under the influence of magnetic field for efficient microprocessor cooling," International Journal of Thermal Sciences, vol. 145, p. 106019, 2019/11/01/ 2019.
36. M. S. Islam, M. M. Hasan, X. Wang, H. D. Germack, and M. Noor-E-Alam, "A Systematic Review on Healthcare Analytics: Application and Theoretical Perspective of Data Mining," Healthcare, vol. 6, p. 54, 2018.
37. H. A. Obeidat, Y. A. S. Dama, R. A. Abd-Alhameed, Y. F. Hu, R. Qahwaji,
38. J. M. Noras, et al., "A Comparison between Vector Algorithm and CRSS Algorithms for Indoor Localization using Received Signal Strength," The Applied Computational Electromagnetics Society (ACES) Journal, vol. 31, 2016.
39. V. Hombach, K. Meier, M. Burkhardt, E. Kuhn, and N. Kuster, "The dependence of EM energy absorption upon human head modeling at 900 MHz," IEEE Transactions on Microwave Theory and Techniques, vol. 44, pp. 1865-1873, 1996.
40. N. Wertheimer and E. Leeper, "Electrical wiring configurations and childhood cancer," Am J Epidemiol, vol. 109, pp. 273-284, 1979.
41. B. Awada, G. Madi, A. Mohsen, A. Harb, A. Diab, L. Hamawy, et al., "Simulation of the Effect of 5G Cell Phone Radiation on Human Brain," in 2018 IEEE International Multidisciplinary Conference on Engineering Technology (IMCET), 2018, pp. 1-6.
42. R. D. Morris, L. L. Morgan, and D. Davis, "Children Absorb Higher Doses of Radio Frequency Electromagnetic Radiation From Mobile Phones Than Adults," IEEE Access, vol. 3, pp. 2379-2387, 2015.
43. P. Bernardi, M. Cavagnaro, S. Pisa, and E. Piuzzi, "Specific absorption rate and temperature increases in the head of a cellular-phone user," IEEE Transactions on Microwave Theory and Techniques, vol. 48, pp. 1118- 1126, 2000.
44. J. Miyakoshi, "Cellular and Molecular Responses to Radio-Frequency Electromagnetic Fields," Proceedings of the IEEE, vol. 101, pp. 1494-1502, 2013.
45. H. Stockman, "Communication by Means of Reflected Power,"
46. Proceedings of the IRE, vol. 36, pp. 1196-1204, 1948.
47. G. Vannucci, A. Bletsas, and D. Leigh, "A Software-Defined Radio System for Backscatter Sensor Networks," IEEE Transactions on Wireless Communications, vol. 7, pp. 2170-2179, 2008.
48. A. Bletsas, S. Siachalou, and J. N. Sahalos, "Anti-collision backscatter sensor networks," IEEE Transactions on Wireless Communications, vol. 8, pp. 5018-5029, 2009.
49. J. Kimionis, A. Bletsas, and J. N. Sahalos, "Bistatic backscatter radio for power-limited sensor

Publisher: Maharaja Chhatrasal Bundelkhand University, Police Lines Road, Panna Road Chhatarpur (M.P) - 471001

networks," in 2013 IEEE Global Communications Conference (GLOBECOM), 2013, pp. 353-358.

50. UK_Physical_Sciences_Centre, "Plagiarism," D. o. Chemistry, Ed., ed. University of Hull, UK: Higher Education Academy, 2009.
51. D. J. Cook and W. Song, "Ambient Intelligence and Wearable Computing: Sensors on the Body, in the Home, and Beyond," Journal of ambient intelligence and smart environments, vol. 1, pp. 83-86, 2009.
52. K. Hänsel, "Wearable and ambient sensing for well-being and emotional awareness in the smart workplace," presented at the Proceedings of the 2016 ACM International Joint Conference on Pervasive and Ubiquitous Computing: Adjunct, Heidelberg, Germany, 2016.
53. T. Heikkilä, E. Strömmer, S. Kivikunnas, M. Järviluoma, M. Korkalainen,
54. V. Kyllönen, et al., "Low intrusive Ehealth monitoring: human posture and activity level detection with an intelligent furniture network," IEEE Wireless Communications, vol. 20, pp. 57-63, 2013.
55. J. Han, H. Kang, and G. H. Kwon, "Understanding the servicescape of nurse assistive robot: The perspective of healthcare service experience," in 2017 14th International Conference on Ubiquitous Robots and Ambient Intelligence (URAI), 2017, pp. 644-649.
56. C. Subramaniam, A. B. Radhakrishnan, V. R. Somu, H. Chandraskear, and J. Balasubramaniam, "HIPAA Based Predictive Analytics for an Adaptive and Descriptive Mobile Healthcare System," in 2013 Fifth International Conference on Computational Intelligence, Modelling and Simulation, 2013, pp. 148-153.
57. J. H. K. Wong, A. K. Y. Wong, W. W. K. Lin, and T. S. Dillon, "Dynamic buffer tuning: An ambience-intelligent way for digital ecosystem success," in 2008 2nd IEEE International Conference on Digital Ecosystems and Technologies, 2008, pp. 184-191.
58. G. Acampora, D. J. Cook, P. Rashidi, and A. V. Vasilakos, "A Survey on Ambient Intelligence in Healthcare," Proceedings of the IEEE, vol. 101, pp. 2470-2494, 2013.
59. M. Ramkumar, S. S. Catharin, and D. Nivetha, "Survey of Cognitive Assisted Living Ambient System Using Ambient intelligence as a Companion," in 2019 IEEE International Conference on System, Computation, Automation and Networking (ICSCAN), 2019, pp. 1-5.
60. J. Esch, "A Survey on Ambient Intelligence in Healthcare," Proceedings of the IEEE, vol. 101, pp. 2467-2469, 2013.
61. T. Magherini, A. Fantechi, C. D. Nugent, and E. Vicario, "Using Temporal Logic and Model Checking in Automated Recognition of Human Activities for Ambient-Assisted Living," IEEE

Publisher: Maharaja Chhatrasal Bundelkhand University, Police Lines Road, Panna Road Chhatarpur (M.P) - 471001

Transactions on Human-Machine Systems, vol. 43, pp. 509-521, 2013.

62. J. Wan, M. Li, M. O. Grady, X. Gu, M. Alawlaqi, and G. O. Hare, "Time- bounded Activity Recognition for Ambient Assisted Living," IEEE Transactions on Emerging Topics in Computing, pp. 1-1, 2018.
63. P. Rashidi and A. Mihailidis, "A Survey on Ambient-Assisted Living Tools for Older Adults," IEEE Journal of Biomedical and Health Informatics, vol. 17, pp. 579-590, 2013.
64. A. Jayatilaka, Y. Su, and D. C. Ranasinghe, "HoTAAL: Home of social things meet ambient assisted living," in 2016 IEEE International Conference on Pervasive Computing and Communication Workshops (PerCom Workshops), 2016, pp. 1-3.

Publisher: Maharaja Chhatrasal Bundelkhand University, Police Lines Road, Panna Road Chhatarpur (M.P) - 471001